

# Moderately Degenerated Human Intervertebral Disks Exhibit a Less Geometrically Specific Collagen Fiber Orientation Distribution

Roman Dittmar<sup>1,\*</sup> Marc M. van Rijsbergen<sup>1,\*</sup> Keita Ito<sup>1</sup>

<sup>1</sup>Division of Orthopaedic Biomechanics, Department of Biomedical Engineering, Eindhoven University of Technology, Eindhoven, The Netherlands

\* Shared first authorship.

Address for correspondence Keita Ito, MD, ScD, Department of Biomedical Engineering, Eindhoven University of Technology, PO Box 513, GEM-Z 4.115, 5600 MB Eindhoven, The Netherlands (e-mail: k.ito@tue.nl).

Global Spine J 2016;6:439–446.

## Abstract

**Study Design** Collagen fiber orientation analysis in moderately degenerated human cadaveric annulus fibrosus (AF) tissue samples.

**Objective** Little is known about the changes in tissue architecture during early degeneration of intervertebral disks (IVDs). As collagen organization strongly affects the disk function, the objective of this study was to quantify the AF collagen orientation and its spatial distribution in moderately degenerated IVDs (Pfirrmann grade III).

**Methods** AF tissue samples were dissected from four circumferential (anterior, left and right lateral, and posterior) and two radial (outer and inner) locations. Cryosections were imaged using Second Harmonic Generation microscopy, and the collagen fiber orientations per location were determined utilizing a fiber-tracking image analysis algorithm. Also, the proportionality between the fibers aligned in the primary direction versus other oriented fibers was determined.

**Results** Mean collagen fiber angles ranged between 21 and 31 degrees for outer and 15 to 19 degrees for inner AF samples. Mean collagen orientations at circumferential locations were only significantly different from each other at inner anterior and lateral location. Similarly, fiber angles between the outer and inner AF were not significantly different except at the posterior location. Fiber orientation proportionality did not show large variations. Except for a significant difference in outer AF proportionality between posterior and lateral positions, no other differences were observed.

**Conclusion** The results of this study provide the first quantitative evidence that the collagen fiber orientation of moderately degenerated disks exhibits a spatial rather than homogeneous distribution and typical collagen orientation gradients characterizing healthy IVDs are only partially retained.

## Keywords

- ▶ intervertebral disk
- ▶ annulus fibrosus
- ▶ collagen orientation
- ▶ second harmonic generation

## Introduction

Degeneration of intervertebral disks (IVDs), the pads of fibrocartilage located between the vertebral bodies of the spine, is commonly considered a major source of

low back pain.<sup>1</sup> This multifaceted condition involves cell-mediated biochemical and structural changes to the center of the IVD, the nucleus pulposus (NP), and its surrounding ring of tissue, the annulus fibrosus (AF).<sup>1</sup>

received  
May 16, 2015  
accepted after revision  
August 19, 2015  
published online  
September 29, 2015

DOI <http://dx.doi.org/10.1055/s-0035-1564805>.  
ISSN 2192-5682.

© 2016 Georg Thieme Verlag KG  
Stuttgart · New York

License terms



Based on cellular and structural differences, the AF can be further divided into an outer AF (OAF) and an inner AF (IAF).<sup>2</sup> Measured from the disk periphery, the OAF consists of the first 18 lamellae, whereas the IAF comprises the next 20 lamellae.<sup>3</sup> Within each lamella, collagen fibers are oriented with a distinct mean angle of  $\pm 30$  degrees (alternating between lamellae) with respect to the transverse plane of the spine.<sup>2,4,5</sup> As shown by Cassidy et al and Holzapfel et al,<sup>3,4</sup> this angle varies both radially and circumferentially with location, leading to a spatially heterogeneous collagen fiber organization in healthy human AF tissue. Specifically, the collagen fiber angle increases radially from  $\sim 30$  degrees in the OAF to  $\sim 45$  degrees in the IAF,<sup>3</sup> and it also increases circumferentially from  $\sim 30$  degrees at the anterior to  $\sim 50$  degrees at the posterior location,<sup>4</sup> which implies that collagen fibers in healthy AF tissue become increasingly oriented in a vertical direction toward the NP and at the posterior location.

The unique lamellar collagen organization of the AF is affected during IVD degeneration. As disks degenerate, structural damage and injury occur including fissures and tears specifically in the AF.<sup>6</sup> Around these severe annular defects, the collagen architecture is remodeled as part of an attempted repair process. This process is likely governed by extracellular matrix degrading enzymes (e.g., matrix metalloproteinases), as previous studies have found a clear association between matrix metalloproteinase expression and tear formation.<sup>7</sup> Furthermore, degenerated disks are characterized by a less apparent distinction between the NP and the AF due to tissue fibrosis. Consequently, the number of distinct lamellae in the AF decreases, whereas the thickness of the remaining concentric layers increases.<sup>2</sup> Ultimately, in severely degenerated IVDs, such progressive degenerative changes lead to a high annular disorganization of the collagen network (i.e., the spatially heterogeneous collagen fiber organization typically observed in healthy AF tissue is lost in severely degenerated disks).<sup>8</sup>

Computational studies have shown that the biomechanical environment of the AF and consequently of the entire disk are dramatically affected when the fiber orientation is altered as local stresses may increase by 100% and total shear strains, up to 50%.<sup>5,9</sup> Although it is well established that severely degenerated IVDs exhibit a high annular disorganization of their collagen network,<sup>8</sup> less is known about (possible) effects of degeneration on the annular collagen fiber architecture of moderately degenerated IVDs. As mechanics directly influences disk cell metabolism and thus cellular function and survival,<sup>10</sup> the long-term success of novel regenerative therapies aiming at treating early/mild degeneration will likely also depend on a thorough understanding of the biomechanical environment they are exposed to.<sup>11</sup> Furthermore, potential changes to the AF collagen organization may serve as a biomarker for improved diagnosis of moderate IVD degeneration, where with the advent of novel imaging techniques such as diffusion tensor imaging,<sup>12</sup> collagen orientation may potentially be assessed in the clinic.

Hence, the aim of this study was to quantify the AF collagen orientation in moderately degenerated disks (Pfirrmann grade III). Cryosections of AF tissue from human

cadaveric disks were obtained and visualized using second harmonic generation (SHG) microscopy. Images were obtained of samples from four circumferential locations (anterior, left lateral, right lateral, and posterior) and two different radial locations (OAF and IAF). Using a collagen fiber tracking algorithm, the primary collagen fiber orientation per location as well as the proportionality between fibers aligned in the primary direction versus nonprimary oriented fibers was determined.

## Materials and Methods

### Sample Preparation

Cadaveric human lumbar spines (L1–S1) were provided by the Anatomy Department of the University Medical Center Utrecht (Utrecht, The Netherlands) following an Institutional Review Board–approved protocol. T2-weighted magnetic resonance images of the spines were acquired and all IVDs were graded by a senior radiologist of the Polyclinique Saint-Côme (Compiègne, France) according to the Pfirrmann scale.<sup>13</sup> Only grade III disks were utilized for further analysis. In total, seven IVDs (levels L1–L2 and L3–L4) from five different donors (all male, mean age  $62.8 \pm 12$  years) were dissected by cutting transversally underneath the superior end plate using a scalpel. IVD pieces containing both OAF and IAF were dissected by making a vertical incision and cutting transversally above the inferior endplate. For each disk, samples were obtained from the anterior, left and right lateral, and posterior location (**Fig. 1A**). According to Cassidy et al,<sup>3</sup> the OAF consists of the outer 18 lamellae ( $\sim 2$  mm as measured from disk periphery), whereas the IAF comprises the next 20 lamellae (until  $\sim 7$  mm). Hence, specimens were split into an OAF sample and an IAF sample by cutting the dissected IVD piece at 2 mm from the outside using a razor blade (**Fig. 1B**). IAF samples were put into molds with their innermost circumferential surfaces tangent to the faces of the molds. Samples were embedded in cryoglue (Sakura Finetek Europe, Alphen aan den Rijn, The Netherlands) with three 0.3-mm-diameter graphite leads (Pentel, Tokyo, Japan) next to them (**Fig. 2**). These leads were used as markers of each sample when they were taken out of the molds and mounted on the cryotome. After freezing overnight at  $-30^\circ\text{C}$ , the samples were mounted on a cryotome (Fisher Scientific, Amsterdam, The Netherlands), and 50- $\mu\text{m}$ -thick tangential cryosections of the OAF and IAF were obtained.

### Second Harmonic Generation Microscopy

SHG images of the OAF and IAF cryosections were acquired on a Leica TCS SP5X laser scanning microscope (Leica, Wetzlar, Germany) with a  $10\times$ , 0.4 numerical aperture objective and excitation light tuned to 810 nm. The SHG signal was collected through a tunable hybrid detector set to 390 to 420 nm. Tiled scans usually comprising 80 individual SHG images were obtained to cover the entire cryosection.

### Image Registration and Analysis

The SHG images of the acquired tiled scans were stitched into a so-called mosaic image of the entire OAF or IAF cryosection

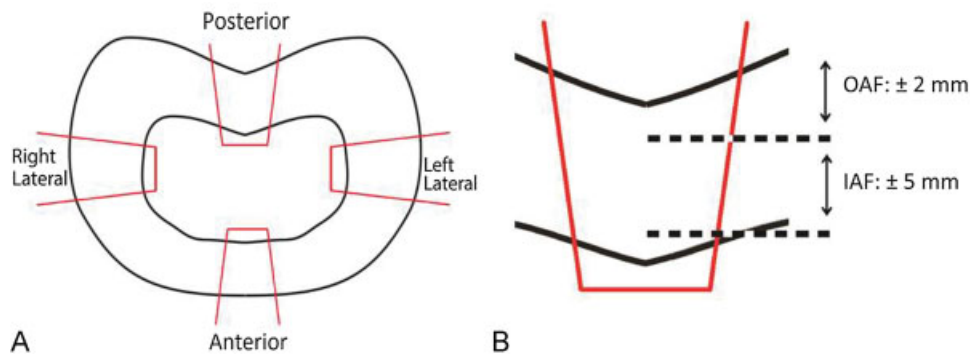


**Fig. 1** Schematic representation of the sample isolation and preparation. (A) Per intervertebral disk (IVD), four wedge-shaped pieces containing both outer annulus fibrosus (OAF) and inner annulus fibrosus (IAF) were dissected. (B) After isolation, each IVD piece (posterior sample shown in schematic) was split in an OAF and IAF sample. Dotted lines represent razor blade dissection sites.

(► **Fig. 3**). As the cryosections were rotated with respect to the transverse plane when placing samples into the cryomolds, the mosaic images had to be first corrected for this rotation prior to further image analysis. Hence, mosaic images were loaded into a custom written Matlab script (Matlab, Natick, Massachusetts, United States). First, the vertical edges of the OAF or IAF sample were defined by manually selecting two points (P1 and P2) located on the edge of the sample (► **Fig. 3A**). Second, three other points (P3, P4, and P5), located equally distributed between these initial two points and on the edge of the sample, were automatically determined. A line was plotted through P1 and P2, then P3 was defined as a point on the sample edge with y-coordinate equal to the center of the plotted line (► **Fig. 3B**). Next, lines through P1 to P3 and P3 to P2 were plotted (► **Fig. 3C**). First, the center points of the lines through P1 to P3 and P3 to P2 were calculated, respectively. Then the points on the sample edge with y-coordinate equal to the center points were defined as P4 and P5 (► **Fig. 3C**). Finally, a line was fitted through all five points using a linear least squares fitting technique (► **Fig. 3D**). The same approach was repeated for the opposite edge of the sample leading to two reference lines with a certain angle with respect to the transverse plane (► **Fig. 3D**). A third, final line was calculated by averaging both reference lines (► **Fig. 3D**). Mosaic images were rotated until this third, final

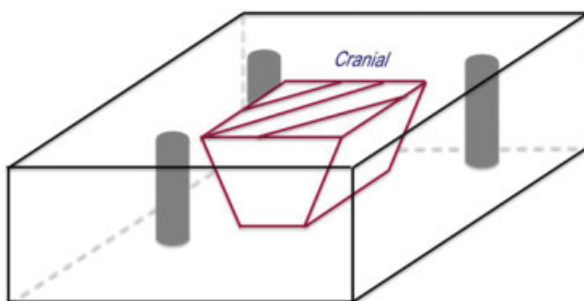


**Fig. 2** Schematic drawing of sample embedding. Each isolated outer annulus fibrosus and inner annulus fibrosus piece was put into a cryomold and embedded in cryogluce. Graphite leads (gray bars) were inserted next to samples.

reference line was aligned in a vertical direction (► **Fig. 3E**). The first mosaic image, into the depth of the section, containing aligned collagen fibers was used for fiber orientation analysis. A subimage was manually cropped out of the mosaic image (► **Fig. 3F**), and an algorithm developed in house was used for quantifying the collagen fiber orientations in the cropped image(s) (► **Fig. 4A**).<sup>14</sup> To make sure the outcome of the manually selected subimage was representative for the entire section, this procedure was repeated at least three times per mosaic image. Care was taken that the subimages were selected from different locations of the mosaic image (i.e., not taken from the same region).

Based on this algorithm, a histogram was created of each sample, and the primary collagen fiber orientation was defined as the angle value with maximum number of counts (► **Fig. 4B**). Collagen fiber angles with an angle value of more than 90 degrees represent the same angle value as the angle minus 90 degrees because no presence of head and or tail could be determined. For the purpose of the current study, both values represent the same direction. Therefore, all results will be given as fiber angle between 0 and 90 degrees. To determine the proportionality of the collagen fibers in the primary direction versus nonprimary directions, as measurement of collagen anisotropy, the root mean square (RMS) of the total counted angle values was used to distinguish between the different orientations. Fiber orientations with counts lower than the RMS were classified as oriented in the nonprimary directions, whereas angles with counts larger than the RMS were identified as fibers in the primary direction (► **Fig. 4B**). This approach was validated by creating multiple idealized distribution ratios (Gaussian-shaped curves) from which the distribution was known and comparing the calculated ratio to the known distribution ratio.

### Statistical Analysis

To determine the differences in fiber primary angles and proportionality between locations, blocked two-way analysis of variance (blocked per disk) was performed followed by Fisher least significant difference post hoc tests for pairwise comparisons between the fiber values and proportionality, respectively. All statistical analysis was performed using SPSS

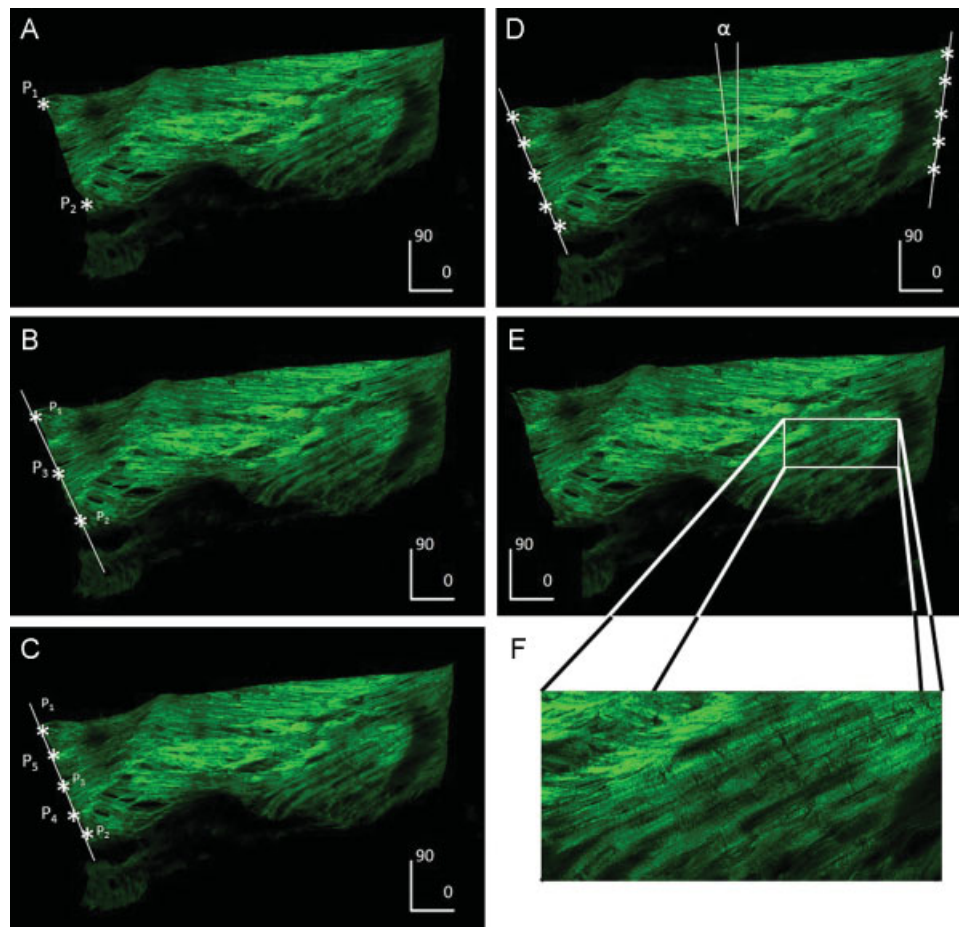


**Fig. 3** Image registration steps. (A) Representative mosaic image prior to registration. Two points, P1 and P2, are manually selected on sample edge. (B) Plotted line through P1 and P2. P3 is automatically determined as point on the sample edge with y-coordinate equal to the line center. (C) P4 and P5 are determined in the same procedure resulting in five equally distributed points on sample edge. (D) Steps described in A to C are repeated on opposite sample edge leading to two reference lines. Average of both reference lines is calculated: third reference line. (E) Mosaic image is rotated until third reference line is aligned in vertical direction. (F) Subimage is cropped out of aligned mosaic image for collagen fiber orientation and proportionality analysis.

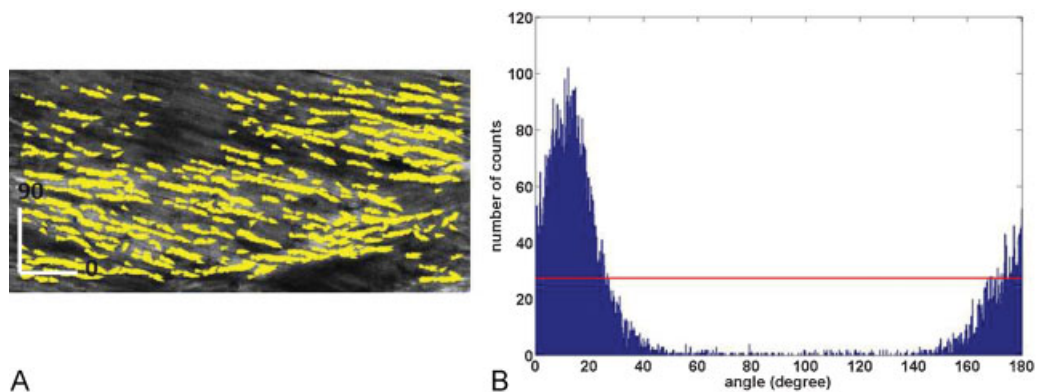


**Fig. 4** (A) Collagen fiber orientation in cropped subimage containing aligned collagen. Yellow arrows indicate calculated fiber orientations. (B) Corresponding histogram of detected fiber orientations; angle values are with respect to the transverse plane. Red line indicates root mean square (RMS) value used for determining proportionality between fibers aligned in primary direction versus nonprimary directions. Fibers having an angle with a count higher than the RMS value were defined as being in the primary directions, whereas fibers having an angle with a count lower than the RMS value were defined as being in the nonprimary directions.

20 (IBM, New York, New York, United States), and statistical significance was assumed for  $p < 0.05$ .

## Results

### Primary Fiber Angle—Outer Annulus Fibrosus

The mean primary collagen fiber angles in the circumferential direction ranged between 21 and 31 degrees for the OAF and exhibited a rather large variance at the posterior position (► **Table 1**). No statistically significant differences were found between the mean primary collagen orientations at the various circumferential locations (► **Fig. 5A**). A trend for increasing mean primary angle from anterior to posterior position was observed, since angle values at anterior and lateral locations showed great similarity and were generally smaller than those at the posterior position.

### Primary Fiber Angle—Inner Annulus Fibrosus

The mean primary collagen fiber angles in the circumferential direction ranged between 15 and 19 degrees for the IAF (► **Table 1**). Significant differences were found between anterior and lateral locations ( $p = 0.032$ ; ► **Fig. 5B**). The mean primary collagen fiber angle values at the lateral and posterior locations were very similar and were larger compared with the anterior location.

### Primary Fiber Angle—Radial Direction

In the radial direction (i.e., from OAF to IAF), the fiber angles did not show strong alterations depending on the position. A radial gradient in collagen orientation was observed only at the posterior location where OAF and IAF angles were significantly different from each other ( $p = 0.008$ ; ► **Fig. 6**).

### Fiber Proportionality

In both the OAF and IAF, the mean primary fiber proportionality was  $70 \pm 20\%$  (► **Table 2**). The OAF samples showed a significantly larger fiber proportionality posteriorly than laterally ( $p = 0.030$ ). No other statistically significant differences in proportionality depending on circumferential locations were observed (► **Table 2**). In contrast, the IAF samples showed very similar mean fiber proportionalities for all circumferential locations, and no statistically significant differences were observed. Also, in the radial direction, no statistically significant differences in the collagen fiber pro-

portionality between the OAF and IAF at the various locations were found.

## Discussion

The unique heterogeneous collagen organization of healthy IVDs was first described in the reports of Cassidy et al and Holzapfel et al.<sup>3,4</sup> They showed that the fiber orientation in the human AF is highly organized and follows strong radial and circumferential gradients. The mean fiber angle increases from the OAF toward the IAF and also depends on the circumferential location within the AF. These established collagen fiber gradients in healthy disks are believed to be essential for proper disk biomechanics and function.<sup>9</sup> Although it is well established that severely degenerated IVDs suffer from a high annular disorganization of their collagen network with presumably detrimental effects to disk function,<sup>1,8,9</sup> our results indicate that the unique AF collagen fiber architecture may already be affected in moderately degenerated disks. Pfirrmann grade III disks observed in this study had a more homogenous AF collagen architecture and only partially retained the collagen orientation gradients typical found in healthy IVDs.

This less organized collagen architecture potentially is also consistent with collagen remodeling and the progressive structural changes observed during degeneration. Such changes include dehydration of the NP, loss of distinction between AF and NP due to tissue fibrosis, and in later stages, the appearance of AF cracks and fissures.<sup>1</sup> With increasing degeneration these cell-mediated degenerative processes affect the lamellar organization of the AF. As the transition between NP and AF fades away, degenerated disks are reported to have fewer and thicker lamellae.<sup>2</sup> Also, as the NP becomes dehydrated, disk height and intradiscal pressure decrease causing the lamellae of the IAF to bulge inward, which in turn may affect the load distribution to these lamellae, potentially inducing or accelerating the remodeling of the AF collagen architecture to cope with the altered biomechanical environment. Hence, a decrease of spatial gradients in the collagen fiber orientation of moderately degenerated disks may be explained by cell-mediated degenerative processes that affect disk biomechanics and trigger disk cells to remodel the AF collagen architecture.

In general, our measurements of fiber angles showed a variance of up to 15 degrees at the different locations (► **Fig. 5**, posterior location), similar to studies of healthy AF tissue.<sup>4</sup> As shown by Marchand and Ahmed and Boos et al,<sup>2,15</sup> this large variance may be explained by the natural heterogeneity of the fiber orientations within the AF and is not related to the imaging used or the orientation analysis technique. SHG microscopy has been extensively used to visualize fibrillar collagens and their organization with the resolution and detail of standard histology.<sup>16</sup> The orientation of collagen fibers in the acquired SHG images was successfully quantified (► **Fig. 4**), which further suggests that the determined large variance is of biological origin (i.e., characteristic of [human] degenerated AF tissue). Our results, obtained on moderately degenerated IVDs, showed a somewhat inhomogeneous

**Table 1** Measured primary collagen fiber orientation

	OAF (mean $\pm$ SD)	IAF (mean $\pm$ SD)
Anterior (degrees)	21.0 $\pm$ 8.2	15.4 $\pm$ 2.7
Lateral (degrees)	21.7 $\pm$ 4.2	19.5 $\pm$ 5.0
Posterior (degrees)	31.5 $\pm$ 14.9	19.2 $\pm$ 9.4

Abbreviations: IAF, inner annulus fibrosus; OAF, outer annulus fibrosus; SD, standard deviation.

Note: Measured primary collagen fiber orientation for both OAF and IAF samples at the various circumferential locations. Values are means  $\pm$  standard deviations ( $n = 7$  for anterior and posterior,  $n = 14$  for lateral).

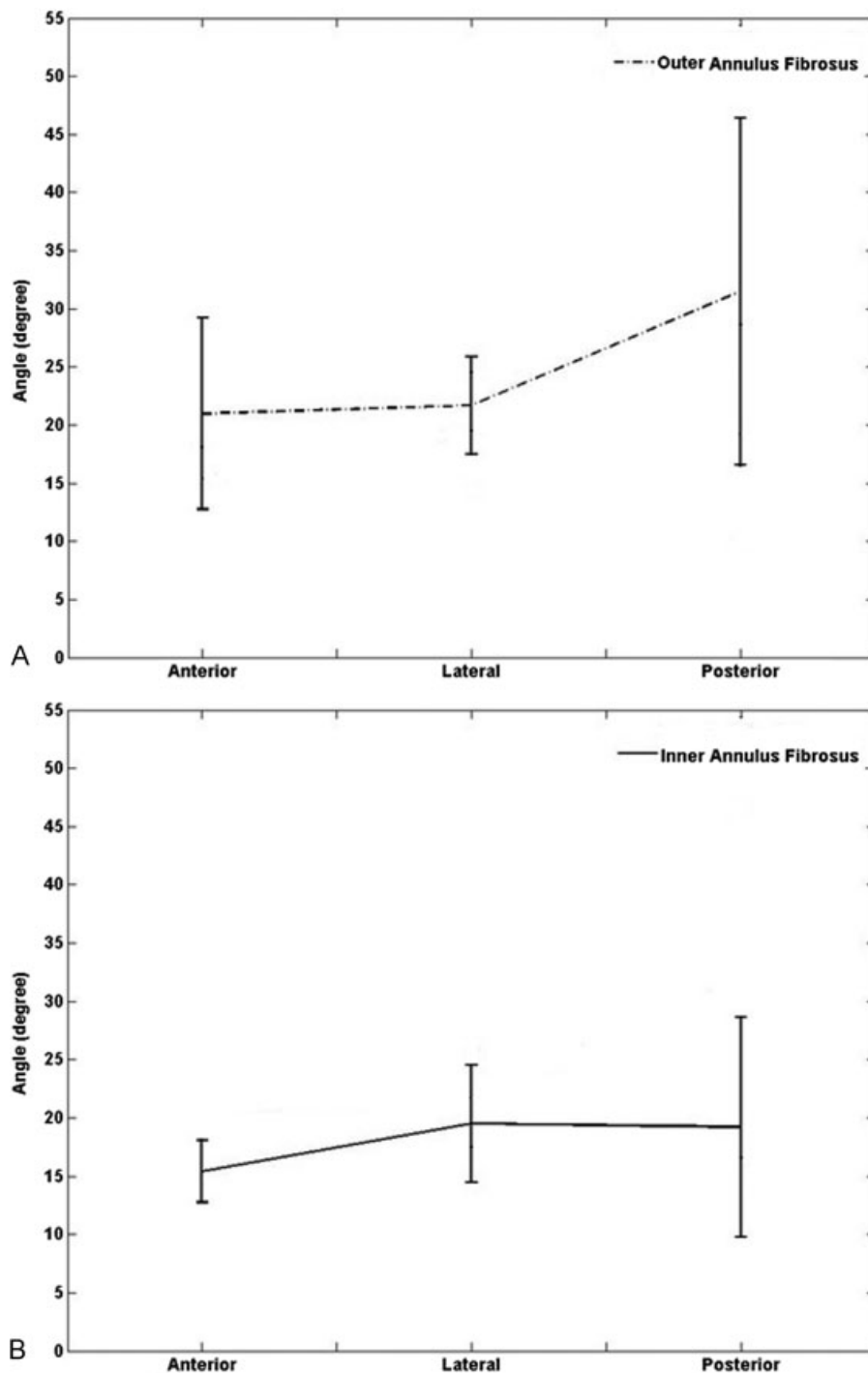


**Fig. 5** Calculated collagen orientations at various circumferential locations. Mean primary collagen fiber orientation for outer annulus fibrosus (A) and inner annulus fibrosus (B) samples at the various circumferential locations. Values are means  $\pm$  standard deviations ( $n = 7$  for anterior and posterior,  $n = 14$  for lateral).

variance distribution where the posterior samples showed larger variance than specimens from other locations, which is likely due to more severe morphological changes of degeneration in AF tissue typically found at the posterior position. Posteriorly, IVDs are much thinner and more prone to injury such as herniation.<sup>4</sup>

As the large variance may have blurred our results, a power analysis on the obtained angle values was conducted. The

calculated power for all comparisons, except for the test between anterior and lateral IAF, was below 80% and, therefore, the sample size would have had to be doubled ( $n = 15$ ) to increase power for all locations (to a minimum of 80%). However, to detect similar differences between the locations as reported for healthy disks, the sample size would also have to be increased, and reports of collagen orientations in healthy AF tissue with a larger sample size ( $n = 11$ ) showed

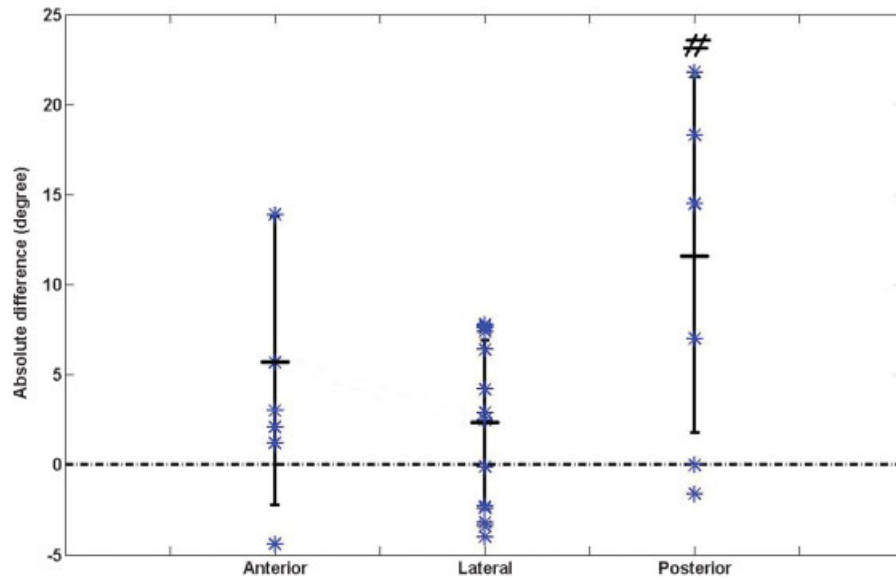


**Fig. 6** Calculated collagen orientations at various radial locations. Absolute difference in primary collagen fiber orientation between outer annulus fibrosus (OAF) and inner annulus fibrosus (IAF) at various circumferential locations. Values are means  $\pm$  standard deviations, including the individual measurements (\* $n = 7$  for anterior and posterior,  $n = 14$  for lateral). At posterior location, a significant difference in fiber orientation between OAF and IAF was determined ( $^{\#}p = 0.008$ ).

similarly large variances.<sup>4</sup> Thus, such large sample sizes are indicative of the observed large variance in collagen fiber orientation of both healthy and moderately degenerated IVDs and not related to the imaging used, image processing technique, or small sample size. This fact suggests that the observed decreased annular organization of moderately degenerated disks is likely a real effect of tissue remodeling and not an artifact due to measuring too few samples.

Decreased spatial heterogeneity in the collagen architecture during moderate degeneration as shown in this study will have implications on disk mechanical behavior and load-bearing function,<sup>4,5</sup> which in turn may induce more or accelerate degenerative changes in the IVD, as the bio-mechanical environment is known to directly influence disk cell metabolism.<sup>10</sup> Elaborate computational models describing healthy IVD mechanics exist that include collagen fiber orientation and also fiber proportionality, as in the case

of Schroeder et al.<sup>17</sup> As other model parameters such as biochemical content (water, proteoglycans, and collagen) are known for degenerated disks, the results of this study may be incorporated to obtain a computational model of a (moderately) degenerated disk, which would further aid in improving the efficacy of novel regenerative medicine approaches (e.g., cell therapy) aiming at treating early degenerated disks. Because the injected cells would be exposed to the same environment that promoted disk degeneration in the first place, a thorough understanding of how altered mechanics due to a more spatially homogenous collagen organization affects disk cell metabolism may increase the long-term success of such regenerative approaches.<sup>11</sup>

In summary, the results of this study provide the first evidence that moderately degenerated IVDs are characterized by a spatially more homogeneous collagen fiber orientation. Typical collagen fiber gradients characterizing healthy IVDs were only partially retained in moderately degenerated human AF tissue. Hence, quantitative data on how degeneration affects collagen architecture specifically in the AF is obtained, which may lead to a better understanding of the mechano-biological environment of moderately degenerated disks. and thus key processes and risk factors involved in disk degeneration may be better understood, potentially leading to improved therapy. Also, these findings may result in an earlier diagnosis of degenerative changes as a more homogenous fiber architecture may serve as a biomarker for moderate disk degeneration.

**Table 2** Measured collagen fiber proportionality

	OAF (mean $\pm$ SD)	IAF (mean $\pm$ SD)
Anterior (%)	70 $\pm$ 9	72 $\pm$ 9
Lateral (%)	66 $\pm$ 12 <sup>a</sup>	71 $\pm$ 9
Posterior (%)	80 $\pm$ 10 <sup>a</sup>	74 $\pm$ 12

Abbreviations: IAF, inner annulus fibrosus; OAF, outer annulus fibrosus; SD, standard deviation.

Note: Collagen fiber proportionality (in %) at various circumferential locations. Values are means  $\pm$  standard deviations ( $n = 7$  for anterior and posterior,  $n = 14$  for lateral).

<sup>a</sup> $p = 0.030$ .

**Disclosures**

Roman Dittmar, Grant: European Research Commission  
 Marc M. van Rijsbergen, Grant: European Research Commission

Keita Ito, Grant: European Research Commission; Board member: AO Foundation

## References

- 1 Urban JP, Roberts S. Degeneration of the intervertebral disc. *Arthritis Res Ther* 2003;5(3):120–130
- 2 Marchand F, Ahmed AM. Investigation of the laminate structure of lumbar disc anulus fibrosus. *Spine (Phila Pa 1976)* 1990;15(5):402–410
- 3 Cassidy JJ, Hiltner A, Baer E. Hierarchical structure of the intervertebral disc. *Connect Tissue Res* 1989;23(1):75–88
- 4 Holzapfel GA, Schulze-Bauer CA, Feigl G, Regitnig P. Single lamellar mechanics of the human lumbar anulus fibrosus. *Biomech Model Mechanobiol* 2005;3(3):125–140
- 5 Guerin HA, Elliott DM. Degeneration affects the fiber reorientation of human annulus fibrosus under tensile load. *J Biomech* 2006;39(8):1410–1418
- 6 Videman T, Nurminen M. The occurrence of anular tears and their relation to lifetime back pain history: a cadaveric study using barium sulfate discography. *Spine (Phila Pa 1976)* 2004;29(23):2668–2676
- 7 Weiler C, Nerlich AG, Zipperer J, Bachmeier BE, Boos N. 2002 SSE Award Competition in Basic Science: expression of major matrix metalloproteinases is associated with intervertebral disc degradation and resorption. *Eur Spine J* 2002;11(4):308–320
- 8 Haefeli M, Kalberer F, Saegesser D, Nerlich AG, Boos N, Paesold G. The course of macroscopic degeneration in the human lumbar intervertebral disc. *Spine (Phila Pa 1976)* 2006;31(14):1522–1531
- 9 Noailly J, Planell JA, Lacroix D. On the collagen criss-cross angles in the annuli fibrosi of lumbar spine finite element models. *Biomech Model Mechanobiol* 2011;10(2):203–219
- 10 Fernando HN, Czamanski J, Yuan TY, Gu W, Salahadin A, Huang CY. Mechanical loading affects the energy metabolism of intervertebral disc cells. *J Orthop Res* 2011;29(11):1634–1641
- 11 Kandel R, Roberts S, Urban JP. Tissue engineering and the intervertebral disc: the challenges. *Eur Spine J* 2008;17(Suppl 4):480–491
- 12 Hsu EW, Setton LA. Diffusion tensor microscopy of the intervertebral disc anulus fibrosus. *Magn Reson Med* 1999;41(5):992–999
- 13 Pfirrmann CW, Metzdorf A, Zanetti M, Hodler J, Boos N. Magnetic resonance classification of lumbar intervertebral disc degeneration. *Spine (Phila Pa 1976)* 2001;26(17):1873–1878
- 14 Daniels F, Ter Haar Romeny BM, Rubbens MP, van Assen H. Quantification of collagen orientation in 3D engineered tissue. In: Ibrahim F, Abu Osman NA, Usman J, Kadri NA, eds. *Biomed 06, IFMBE Proceedings* 15, 2007, pp. 282–286
- 15 Boos N, Weissbach S, Rohrbach H, Weiler C, Spratt KF, Nerlich AG. Classification of age-related changes in lumbar intervertebral discs: 2002 Volvo Award in basic science. *Spine (Phila Pa 1976)* 2002;27(23):2631–2644
- 16 Zipfel WR, Williams RM, Christie R, Nikitin AY, Hyman BT, Webb WW. Live tissue intrinsic emission microscopy using multiphoton-excited native fluorescence and second harmonic generation. *Proc Natl Acad Sci U S A* 2003;100(12):7075–7080
- 17 Schroeder Y, Huyghe JM, van Donkelaar CC, Ito K. A biochemical/biophysical 3D FE intervertebral disc model. *Biomech Model Mechanobiol* 2010;9(5):641–650